

Title	Passivation of textured crystalline silicon surfaces by catalytic CVD silicon nitride films and catalytic phosphorus doping
Author(s)	Ohdaira, Keisuke; Cham, Trinh Thi; Matsumura, Hideki
Citation	Japanese Journal of Applied Physics, 56(10): 102301-1-102301-4
Issue Date	2017-09-11
Type	Journal Article
Text version	author
URL	<a href="http://hdl.handle.net/10119/15424">http://hdl.handle.net/10119/15424</a>
Rights	This is the author's version of the work. It is posted here by permission of The Japan Society of Applied Physics. Copyright (C) 2017 The Japan Society of Applied Physics. Keisuke Ohdaira, Trinh Thi Cham and Hideki Matsumura, Japanese Journal of Applied Physics, 56(10), 2017, 102301-1-102301-4. <a href="http://dx.doi.org/10.7567/JJAP.56.102301">http://dx.doi.org/10.7567/JJAP.56.102301</a>
Description	

# **Passivation of textured crystalline silicon surfaces by catalytic CVD silicon nitride films and catalytic phosphorus doping**

Keisuke Ohdaira<sup>\*</sup>, Trinh Thi Cham<sup>†</sup>, and Hideki Matsumura

*Japan Advanced Institute of Science and Technology, Nomi, Ishikawa 923-1292, Japan*

<sup>\*</sup>E-mail: ohdaira@jaist.ac.jp

<sup>†</sup>Present address: Helmholtz-Zentrum Berlin für Materialien und Energie, D-12489 Berlin, Germany

Silicon nitride ( $\text{SiN}_x$ ) films formed by catalytic chemical vapor deposition (Cat-CVD) and phosphorus-doped layers formed by catalytic impurity doping (Cat-doping) are applied for the passivation of pyramid-shaped textured crystalline Si (c-Si) surfaces formed by anisotropic etching in alkaline solution. Lower surface recombination velocities (SRVs) tend to be obtained when smaller pyramids are formed on c-Si surfaces. Phosphorus Cat-doping is effective for reducing the SRV of textured c-Si surfaces as in the case of flat c-Si surfaces. We realize SRVs of textured c-Si surfaces of  $\sim 8.0$  and  $\sim 6.7$  cm/s for only  $\text{SiN}_x$  passivation and for the combination of  $\text{SiN}_x$  and P Cat-doping, respectively. These structures also have optical transparency and low Auger recombination loss, and are of great worth in application for the surface passivation of interdigitated back-contact c-Si solar cells.

## 1. Introduction

Global photovoltaic (PV) market has been expanding owing to the concern about the issue of long-term energy supply. The present share of PV-based electricity in the global electricity demand is only ~1%,<sup>1)</sup> and the usage of PV technologies must be further accelerated. The important point to achieve more PV-based electricity is to increase the conversion efficiency of crystalline silicon (c-Si) solar cells and modules, which occupy the current PV market share of ~90%.<sup>1)</sup> Among a variety of c-Si solar cell structures, interdigitated back-contact (IBC) solar cells have attracted much attention because of their high-efficiency potential owing to the absence of shading loss originating from surface metal electrodes.<sup>2-7)</sup> All the recent breakages of efficiency records in c-Si solar cells have been achieved by c-Si cells with the IBC structures, some of which consist of amorphous Si (a-Si)/c-Si heterostructures.<sup>4,5)</sup> In the IBC solar cells, the quality of illuminated-side surface passivation films is of particular importance, since photogenerated carriers generated near the front-side surface must reach the doping layers formed on the rear-side surface through long-distance diffusion for the contribution to power generation. Another important factor required for the surface passivation films is sufficient optical transparency, because parasitic absorption in the passivation layer significantly reduces the number of photons entering into the c-Si absorber. In addition to the passivation effect brought from the surface layer, a highly phosphorus (P)-doped region on the surface of c-Si for field-effect passivation is also often used to further reduce the recombination of photogenerated carriers. The highly doped layer, however, also induces Auger recombination, and it should thus be as thin as possible.

Catalytic chemical vapor deposition (Cat-CVD) is a method of depositing thin films through the catalytic decomposition of gas molecules on a heated catalyzing wire. Owing to this feature, Cat-CVD can realize the plasma-damage-less deposition of thin films such as a-Si and Si nitride ( $\text{SiN}_x$ ), and produce high-quality films for the passivation of c-Si surfaces.<sup>8-16)</sup> We have thus far realized Cat-CVD  $\text{SiN}_x$  passivation films showing a surface recombination velocity (SRV) of ~5 cm/s on mirror-polished c-Si(100) surfaces.<sup>12)</sup> It should be emphasized that the  $\text{SiN}_x$  films are stoichiometric and have a refractive index of ~2, leading to no parasitic absorption of sunlight. A Cat-CVD system can also be utilized to dope boron or P atoms to c-Si surfaces through the catalytic cracking of  $\text{PH}_3$  or  $\text{B}_2\text{H}_6$

gas molecules.<sup>17–27)</sup> We have referred this newly developed doping method as catalytic impurity doping (Cat-doping). The formation of a P Cat-doped layer on the surfaces of c-Si wafers contributes to the further reduction in an SRV, and SiN<sub>x</sub>/P Cat-doped layer stacks realize an SRV of ~2 cm/s on mirror-polished Si(100) surfaces.<sup>22)</sup> Fortunately, the thickness of a P Cat-doped layer is as small as <10 nm,<sup>23)</sup> and the harmful influence of a highly doped region—Auger recombination—can thus be minimized.

These excellent SRVs have been obtained only on mirror-polished flat c-Si surfaces thus far. In actual c-Si solar cells including IBC cells, a pyramid-shaped textured structure is generally formed through the anisotropic etching of Si(100) wafers in alkaline solution on their surfaces to suppress optical reflectance. For the application of the Cat-CVD-related passivation structures to actual IBC cells, their availability on textured c-Si surfaces must be demonstrated. In this paper, we have investigated the potential of Cat-CVD SiN<sub>x</sub> films and P Cat-doping for the passivation of pyramid-shaped c-Si surfaces. Markedly low SRVs of 8.0 and 6.7 cm/s are realized for SiN<sub>x</sub> and SiN<sub>x</sub>/P Cat-doped layer structures, respectively, which are applicable to the surface passivation of IBC cells.

## 2. Experimental methods

We used 290- $\mu$ m-thick, double-side mirror-polished n-type c-Si(100) wafers, which have a resistivity of 1–5  $\Omega$ ·cm and a bulk minority carrier lifetime ( $\tau_b$ ) of >10 ms. The wafers were first cleaved to 20 $\times$ 20 mm<sup>2</sup>-sized small pieces, and then dipped in 5% hydrofluoric acid (HF) to remove native oxide layers. After the ultrasonic cleaning in deionized water, the wafers were immersed in a mixture of deionized water and KOH-based alkaline solution, SUN-X 600 (Wako Pure Chemical Industries), with a ratio of 3:1 to form pyramid-shaped textures through anisotropic etching. The texturing process was performed at temperatures of 60–90 °C for various durations up to 50 min. The textured c-Si wafers were cleaned through so-called “RCA cleaning”, in which we used NH<sub>4</sub>OH:H<sub>2</sub>O<sub>2</sub>:H<sub>2</sub>O=1:1:5 solution (SC-1) for 15 min to remove organic impurities, and then HCl:H<sub>2</sub>O<sub>2</sub>:H<sub>2</sub>O=1:1:5 solution (SC-2) for 15 min to remove metallic contaminants.<sup>28)</sup> Mirror-polished Si(100) and Si(111) substrates with a  $\tau_b$  of >10 ms without alkali etching were also used as reference samples.

We then deposited SiN<sub>x</sub> films on both sides of the c-Si wafers by Cat-CVD, in which

a heated tungsten wire was used as a catalyzer. The deposition conditions of the SiN<sub>x</sub> films, including substrate temperature ( $T_{\text{sub}}$ ), catalyzer temperature ( $T_{\text{cat}}$ ), catalyzer–substrate distance ( $D_{\text{cs}}$ ), pressure, duration, and gas flow rate, are summarized in Table I, under which ~100-nm-thick SiN<sub>x</sub> films were formed if flat substrates were used. Spectroscopic ellipsometry measurement and analysis by the Cauchy model revealed that the SiN<sub>x</sub> films have a refractive index of ~2 and a negligible extinction coefficient even in a short wavelength region. Part of the c-Si wafers received P Cat-doping on their both sides under the conditions summarized in Table I, prior to the deposition of the SiN<sub>x</sub> films. In the P Cat-doping, PH<sub>3</sub> molecules are known to be catalytically decomposed to P and H radicals on a tungsten catalyzer.<sup>29,30</sup> The samples with SiN<sub>x</sub> films were then annealed at 350 °C for 30 min under N<sub>2</sub> atmosphere in a tube furnace to enhance the termination of dangling bonds on c-Si surfaces by hydrogen atoms supplied from SiN<sub>x</sub> films for improvement in passivation quality.<sup>12,16</sup> After the postannealing, the SiN<sub>x</sub> films show a fixed charge density of  $7 \times 10^{11} / \text{cm}^2$  and an interface state density of  $3.1 \times 10^{11} / \text{cm}^2$ .<sup>16</sup>

The surface morphology of the textured c-Si wafers was observed by scanning electron microscopy (SEM). The optical reflectance spectra of uncoated and SiN<sub>x</sub>-coated c-Si wafers before and after texturing were measured in a spectrophotometer (Shimadzu UV-3150) equipped with an integrating sphere. The quality of the passivation structures was evaluated by measuring the effective minority carrier lifetime ( $\tau_{\text{eff}}$ ) using the microwave photoconductivity decay ( $\mu$ -PCD) (Kobelco Research Institute LTA-1510EP). A pulse laser with a wavelength of 904 nm and an areal photon density of  $5 \times 10^{13} / \text{cm}^2$  was used for the generation of excess carriers in c-Si. The SRV of c-Si surfaces was evaluated using the following equation:

$$\tau_{\text{eff}}^{-1} = \tau_{\text{b}}^{-1} + 2S/W, \quad (1)$$

where  $S$  and  $W$  represent SRV and wafer thickness, respectively.  $\tau_{\text{b}}$  of c-Si used in this study was considerably high, as mentioned above, and we neglected the term  $\tau_{\text{b}}^{-1}$  and obtained  $S$  simply from  $W$  and measured  $\tau_{\text{eff}}$ . Note that SRV obtained from this procedure corresponds to the maximum SRV for the measured  $\tau_{\text{eff}}$ .

### 3. Results and discussion

Pyramid structures formed through alkaline etching have (111)-oriented facets. If the SRVs of textured Si surfaces differ from those of flat Si(100) wafers, two factors—surface roughness and surface orientation—should be discussed separately. We thus first compared the passivation quality of Cat-CVD SiN<sub>x</sub> films on flat Si(100) and Si(111) substrates. Figure 1 shows the SRVs of the mirror-polished Si(100) and Si(111) substrates passivated with SiN<sub>x</sub> films and SiN<sub>x</sub>/P Cat-doped layer stacks. Low SRVs of ~5 and ~2 cm/s are obtained on mirror-polished Si(100) surfaces passivated with SiN<sub>x</sub> films and SiN<sub>x</sub>/P Cat-doped layer stacks, respectively, as have been reported.<sup>12,22)</sup> Considerably low SRVs of ~6.5 and ~3 cm/s can be similarly obtained also on Si(111) by the passivation using SiN<sub>x</sub> films and SiN<sub>x</sub>/P Cat-doped layer stacks, respectively, although the SRVs are slightly higher than those on Si(100) surfaces. We here conclude that Cat-CVD SiN<sub>x</sub> films have sufficient passivation quality on Si(111) surfaces, and P Cat-doping prior to the deposition of SiN<sub>x</sub> films is effective to additionally reduce the SRV of Si(111) surfaces. The slightly worse passivation quality on Si(111) than on Si(100) has also been reported in a previous literature based on the results of SiN<sub>x</sub> films formed by plasma-enhanced CVD;<sup>31)</sup> however, the reason for it is unclear.

Figure 2 shows the SEM images of c-Si surfaces formed through alkaline etching for 50 min at different solution temperatures. The formation of Si(111)-faceted pyramids is confirmed on all the c-Si samples. The size of pyramids strongly depends on temperature during alkaline etching, and larger pyramids tend to be formed at higher alkaline solution temperatures. Figure 3 shows the SRVs of SiN<sub>x</sub>/textured c-Si interfaces as a function of temperature during alkaline etching. Sufficiently low SRVs of <10 cm/s are obtained on c-Si surfaces textured at ≤70 °C, while the passivation of c-Si surfaces textured at higher temperatures results in much worse SRV. This fact indicates that the passivation ability of Cat-CVD SiN<sub>x</sub> films significantly depends on the morphology of c-Si surfaces, and smaller pyramids seem to result in a lower SRV. This might be due to the insufficient coverage of c-Si surfaces with SiN<sub>x</sub> films particularly around deeper valleys existing between large pyramids. The control of the size of pyramids is thus important to realize sufficiently low SRV.

Figure 4(a) shows the optical reflectance spectra of c-Si surfaces textured in the

alkaline solution at 70 °C for various durations up to 50 min before SiN<sub>x</sub> deposition. The optical reflectance of the c-Si samples decreases monotonically with increasing alkali etching duration at all the wavelengths. This results from the formation of pyramid-shaped textures on the c-Si surfaces. An optical reflectance of ~10% obtained after 50 min of alkali etching at a wavelength of 600 nm is a typical value for alkali-textured c-Si surfaces, indicating a sufficient light-trapping effect of surface textured structures. Figure 4(b) shows the texturing-duration dependence of the optical reflectance spectra of the c-Si surfaces after SiN<sub>x</sub> deposition. The optical reflectance of the samples largely decreases, compared with those of the c-Si wafers without SiN<sub>x</sub> films, owing to the antireflection effect of the SiN<sub>x</sub> films. In particular, optical reflectance <5% in a wide wavelength region is realized in the case of 50-min alkali etching, which is applicable to the antireflection surface structure on the illuminated side of actual solar cells. Note that the non-negligible reflectance in a wavelength region of 400–600 nm in the reflectance spectrum is due to unoptimized SiN<sub>x</sub> thickness. Figure 5 shows the SRVs of c-Si surfaces passivated with SiN<sub>x</sub> films as a function of texturing duration. SRV increases with an increase in alkaline etching duration; however, an SRV of <10 cm/s can be obtained for the sample receiving 50-min alkaline etching, under which optical reflectance is fully reduced. One reason for the increase in SRV must be the enlargement of the surface area of c-Si by the formation of pyramid structures. Other possible reasons might be the existence of a partially uncovered region on c-Si surfaces and slightly less effective passivation ability on Si(111) surfaces, as shown in Fig. 1.

Figure 6 shows the SRVs of flat Si(100) and textured c-Si surfaces passivated with SiN<sub>x</sub> films and SiN<sub>x</sub>/P Cat-doped layer stacks. The textured c-Si wafers were formed through etching in the alkaline solution for 50 min at 70 °C. The textured wafer passivated with SiN<sub>x</sub>/P Cat-doped layer stacks shows an SRV of ~6.7 cm/s, which is smaller than that of the textured c-Si passivated with SiN<sub>x</sub> films of ~8.0 cm/s. This fact indicates that P Cat-doping is effective also for textured c-Si surfaces. The effect of P Cat-doping on the reduction in the SRV is, however, less significant on textured c-Si surfaces than on flat c-Si surfaces. This might be due to the less efficiency of P Cat-doping particularly in the vicinity of the valleys of pyramids, at which the number of P radicals must be smaller than that at the top of pyramids.

The SRVs of 6.7 and 8.0 cm/s obtained by using Cat-CVD SiN<sub>x</sub> films and P Cat-doping are still excellent values and are on the available level for the surface passivation of IBC solar cells. It should be emphasized that there is no serious parasitic absorption of sunlight in the SiN<sub>x</sub> used here, unlike the case of a-Si or Si-rich SiN<sub>x</sub> films with a high absorption coefficient.<sup>8-10)</sup> Negligible Auger recombination loss in the ultrathin P Cat-doped layer is another advantage of the present passivation structures in comparison with conventional P doping through thermal diffusion using POCl<sub>3</sub> leading to the formation of >100-nm-thick highly doped layers. The application of Cat-CVD SiN<sub>x</sub> films and P Cat-doping would lead to the further improvement in the performance of IBC solar cells.

#### **4. Conclusions**

We have applied Cat-CVD SiN<sub>x</sub> films and P Cat-doping for the passivation of the surfaces of c-Si with (111)-faceted pyramid-shaped textured structures formed through alkali etching. Si(111) mirror-polished wafers passivated with SiN<sub>x</sub> films and SiN<sub>x</sub>/P Cat-doped layer stacks show significantly low SRVs similar to the case of Si(100) surfaces, indicating the effectiveness of the Cat-CVD SiN<sub>x</sub> films and Cat-doping for the passivation of Si(111) surfaces. Textured c-Si surfaces with smaller pyramids tend to show lower SRV by passivation with Cat-CVD SiN<sub>x</sub> films, and an SRV of ~8.0 cm/s can be obtained when a c-Si surface has pyramids with an appropriate size. The addition of P Cat-doping to the textured c-Si surfaces results in a much lower SRV of ~6.7 cm/s. These passivation structures will be applied to the illuminated-side surface passivation of IBC solar cells.

#### **Acknowledgments**

This work was supported by the Core Research for Evolutional Science and Technology (CREST), Japan Science and Technology Agency (JST) program.



## References

- 1) Trends 2015 in Photovoltaic Applications  
[[http://www.iea-pvps.org/fileadmin/dam/public/report/national/IEA-PVPS\\_-\\_Trends\\_2015\\_-\\_MedRes.pdf](http://www.iea-pvps.org/fileadmin/dam/public/report/national/IEA-PVPS_-_Trends_2015_-_MedRes.pdf)].
- 2) D. D. Smith, P. Cousins, S. Westerberg, R. De Jesus-Tabajonda, G. Aniero, and Y.-C. Shen, *IEEE J. Photovoltaics* **4**, 1465 (2014).
- 3) J. Nakamura, N. Asano, T. Hieda, C. Okamoto, H. Katayama, and K. Nakamura, *IEEE J. Photovoltaics* **4**, 1491 (2014).
- 4) K. Masuko, M. Shigematsu, T. Hashiguchi, D. Fujishima, M. Kai, N. Yoshimura, T. Yamaguchi, Y. Ichihashi, T. Mishima, N. Matsubara, T. Yamanishi, T. Takahama, M. Taguchi, E. Maruyama, and S. Okamoto, *IEEE J. Photovoltaics* **4**, 1433 (2014).
- 5) K. Yoshikawa, H. Kawasaki, W. Yoshida, T. Irie, K. Konishi, K. Nakano, T. Uto, D. Adachi, M. Kanematsu, H. Uzu, and K. Yamamoto, *Nat. Energy* **2**, 17032 (2017).
- 6) G. Yang, A. Ingenito, O. Isabella, and M. Zeman, *Sol. Energy Mater. Sol. Cells* **158**, 84 (2016).
- 7) G. Xu, Y. Yang, X. Zhang, S. Chen, W. Liu, Y. Chen, Z. Li, Y. Chen, P. P. Altermatt, P. J. Verlinden, and Z. Feng, *Proc. 43rd IEEE Photovoltaic Specialists Conf.*, 2016, p. 3356.
- 8) K. Koyama, K. Ohdaira, and H. Matsumura, *Appl. Phys. Lett.* **97**, 082108 (2010).
- 9) K. Koyama, K. Ohdaira, and H. Matsumura, *Thin Solid Films* **519**, 4473 (2011).
- 10) T. C. Thi, K. Koyama, K. Ohdaira, and H. Matsumura, *Sol. Energy Mater. Sol. Cells* **100**, 169 (2012).
- 11) K. Higashimine, K. Koyama, K. Ohdaira, H. Matsumura, and N. Otsuka, *J. Vac. Sci. Technol. B* **30**, 031208 (2012).
- 12) T. C. Thi, K. Koyama, K. Ohdaira, and H. Matsumura, *Jpn. J. Appl. Phys.* **53**, 022301 (2014).
- 13) T. C. Thi, K. Koyama, K. Ohdaira, and H. Matsumura, *Thin Solid Films* **575**, 60 (2015).
- 14) T. Oikawa, K. Ohdaira, K. Higashimine, and H. Matsumura, *Current Appl. Phys.* **15**, 1168 (2015).
- 15) K. Ohdaira, T. Oikawa, K. Higashimine, and H. Matsumura, *Current Appl. Phys.* **16**, 1026 (2016).
- 16) T. C. Thi, K. Koyama, K. Ohdaira, and H. Matsumura, *Jpn. J. Appl. Phys.* **55**, 02BF09

(2016).

- 17) H. Matsumura, M. Miyamoto, K. Koyama, and K. Ohdaira, *Sol. Energy Mater. Sol. Cells* **95**, 797 (2011).
- 18) T. Hayakawa, Y. Nakashima, M. Miyamoto, K. Koyama, K. Ohdaira, and H. Matsumura, *Jpn. J. Appl. Phys.* **50**, 121301 (2011).
- 19) T. Hayakawa, Y. Nakashima, K. Koyama, K. Ohdaira, and H. Matsumura, *Jpn. J. Appl. Phys.* **51**, 061301 (2012).
- 20) T. Hayakawa, M. Miyamoto, K. Koyama, K. Ohdaira, and H. Matsumura, *Thin Solid Films* **519**, 4466 (2011).
- 21) T. Hayakawa, T. Ohta, Y. Nakashima, K. Koyama, K. Ohdaira, and H. Matsumura, *Jpn. J. Appl. Phys.* **51**, 101301 (2012).
- 22) T. C. Thi, K. Koyama, K. Ohdaira, and H. Matsumura, *J. Appl. Phys.* **116**, 044510 (2014).
- 23) H. Matsumura, T. Hayakawa, T. Ohta, Y. Nakashima, M. Miyamoto, T. C. Thi, K. Koyama, and K. Ohdaira, *J. Appl. Phys.* **116**, 114502 (2014).
- 24) T. Ohta, K. Koyama, K. Ohdaira, and H. Matsumura, *Thin Solid Films* **575**, 92 (2015).
- 25) S. Tsuzaki, K. Ohdaira, T. Oikawa, K. Koyama, and H. Matsumura, *Jpn. J. Appl. Phys.* **54**, 072301 (2015).
- 26) J. Seto, K. Ohdaira, and H. Matsumura, *Jpn. J. Appl. Phys.* **55**, 04ES05 (2016).
- 27) K. Ohdaira, J. Seto, and H. Matsumura, *Jpn. J. Appl. Phys.* **56**, 08MB06 (2017).
- 28) W. Kern and D. Puotmen, *RCA Rev.* **31**, 187 (1970).
- 29) H. Umemoto, Y. Nishihara, T. Ishikawa, and S. Yamamoto, *Jpn. J. Appl. Phys.* **51**, 086501 (2012).
- 30) H. Umemoto, T. Kanemitsu, and Y. Kuroda, *Jpn. J. Appl. Phys.* **53**, 05FM02 (2014).
- 31) F. M. Schuurmans, A. Schonecker, J. A. Eikelboom, and W. C. Sinke, *Proc. 25th IEEE Photovoltaic Specialists Conf.*, 2002, p. 485.

## Figure Captions

**Fig. 1.** SRVs of the mirror-polished Si(100) and Si(111) passivated with SiN<sub>x</sub> films and SiN<sub>x</sub>/P Cat-doped layer stacks.

**Fig. 2.** SEM images of c-Si surfaces after alkaline etching for 50 min at (a) 65, (b) 70, and (c) 80 °C.

**Fig. 3.** SRVs of SiN<sub>x</sub>/textured c-Si interfaces as a function of temperature during texturing.

**Fig. 4.** (Color online) Optical reflectance spectra of c-Si surfaces textured in alkaline solution at 70 °C for various durations (a) without and (b) with SiN<sub>x</sub> films.

**Fig. 5.** (Color online) SRVs of c-Si surfaces passivated with SiN<sub>x</sub> films as a function of the duration of alkaline texturing.

**Fig. 6.** (Color online) SRVs of flat and textured c-Si surfaces passivated with SiN<sub>x</sub> films or a SiN<sub>x</sub>/P Cat-doped layer stacks.

Table I. Conditions for SiN<sub>x</sub> deposition by Cat-CVD and P Cat-doping.

	$T_{\text{sub}}$ (°C)	$T_{\text{cat}}$ (°C)	$D_{\text{cs}}$ (cm)	Pressure (Pa)	Gas	Flow rate (sccm)	Duration (s)
SiN <sub>x</sub> deposition	100	1800	8	10	SiH <sub>4</sub> NH <sub>3</sub>	8 150	184
P Cat-doping	80	1800	12	1.0	2.25% PH <sub>3</sub> (He-diluted)	20	60

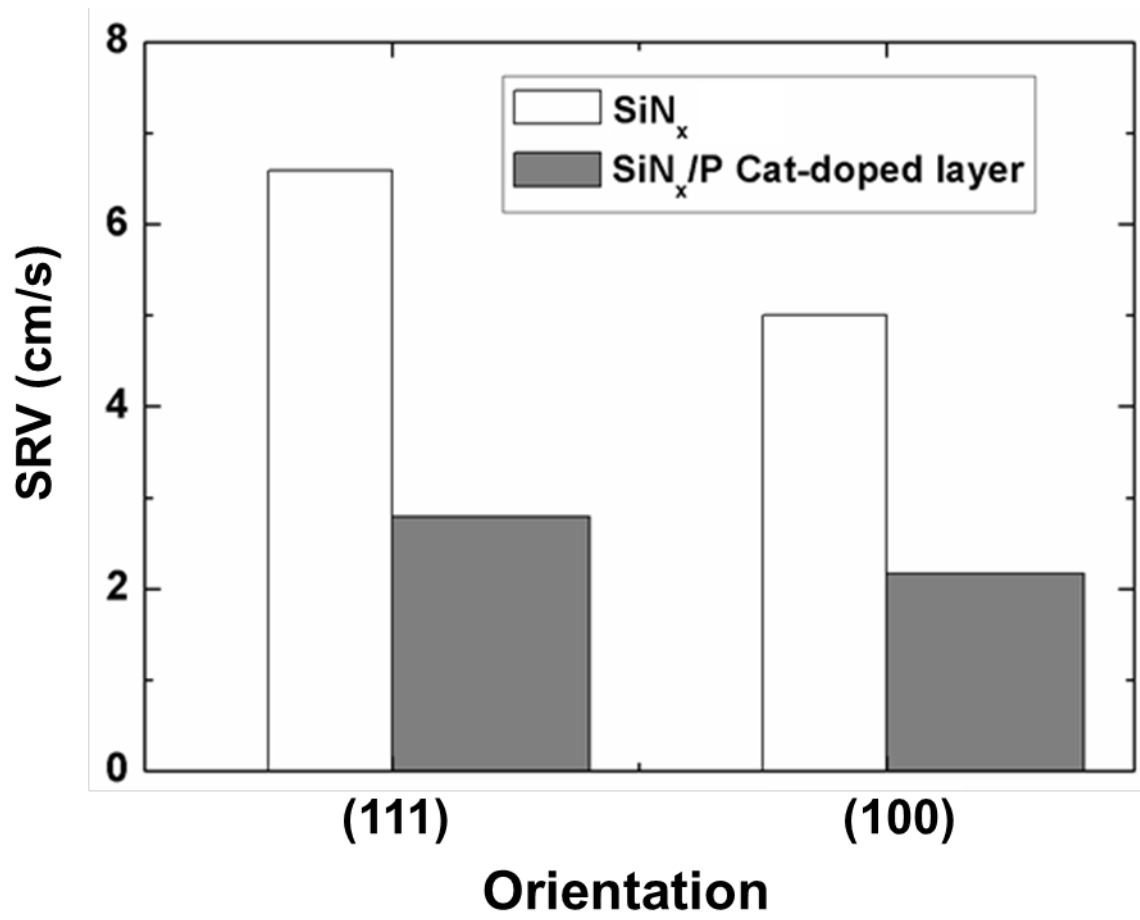


Fig. 1.

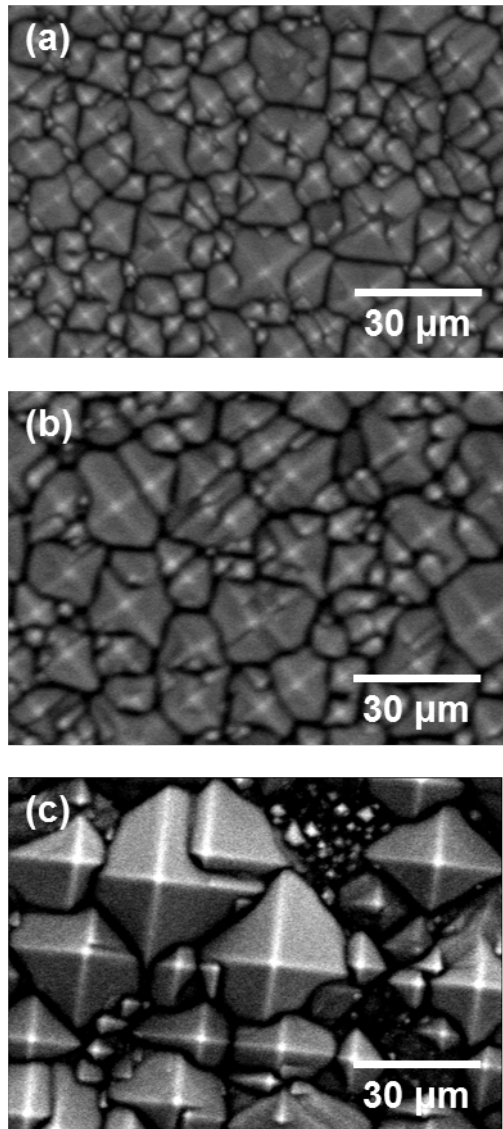


Fig. 2.

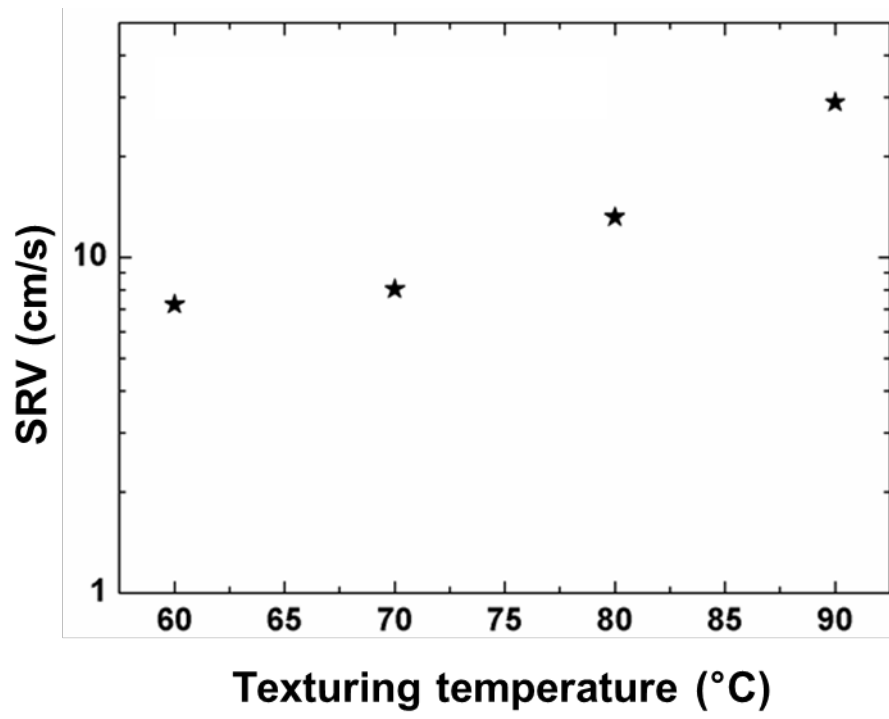


Fig. 3.

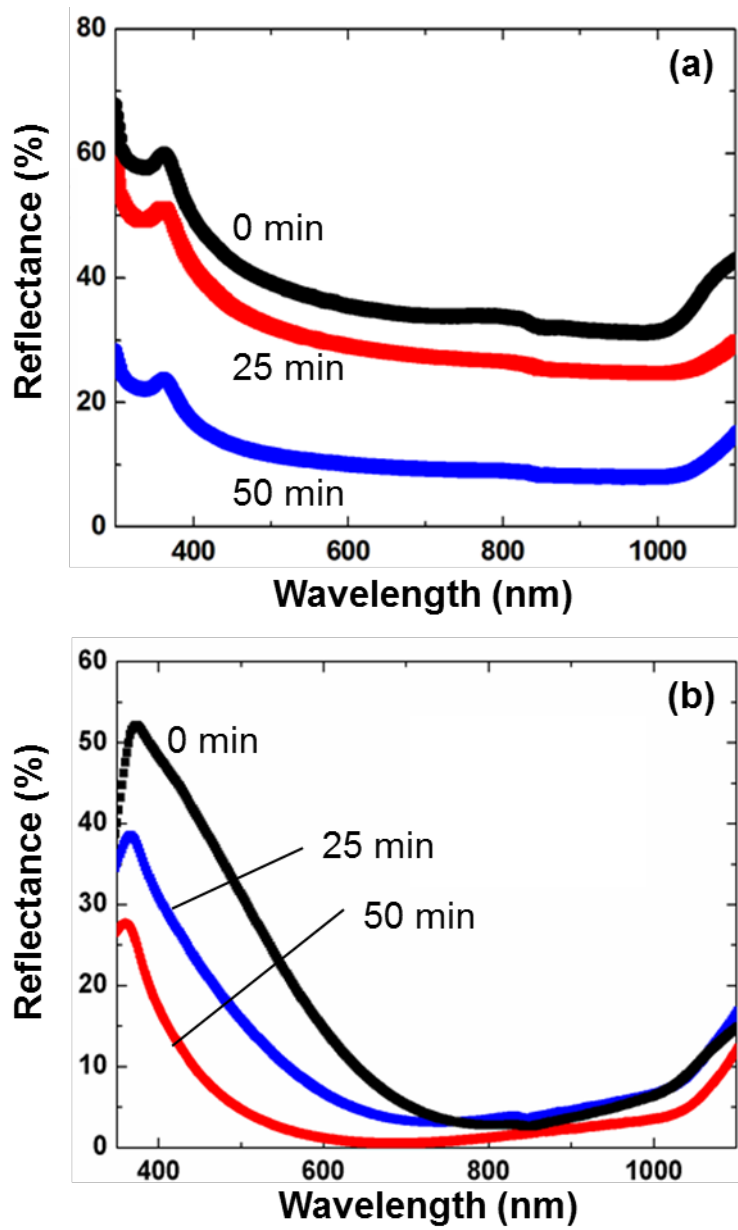


Fig. 4. (Color online)



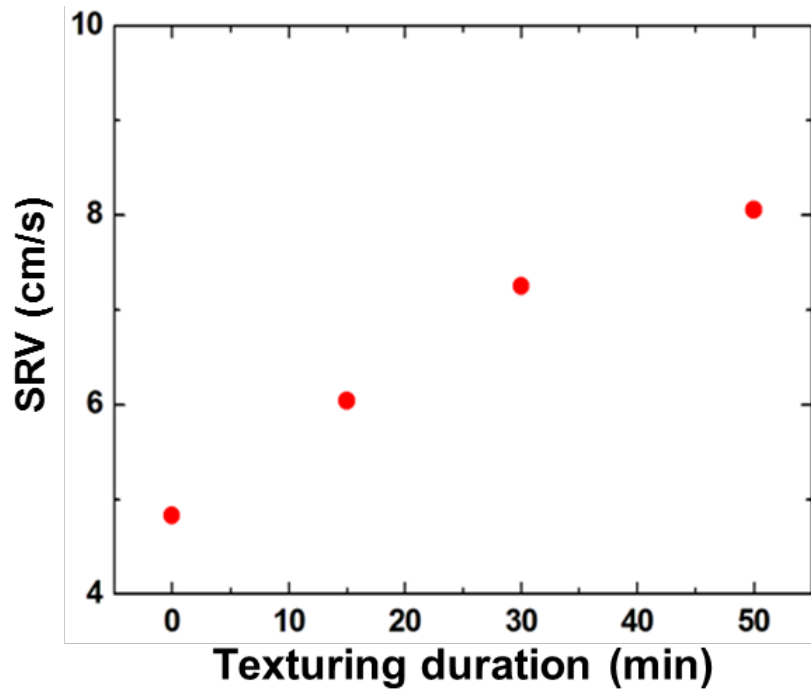


Fig. 5. (Color online)

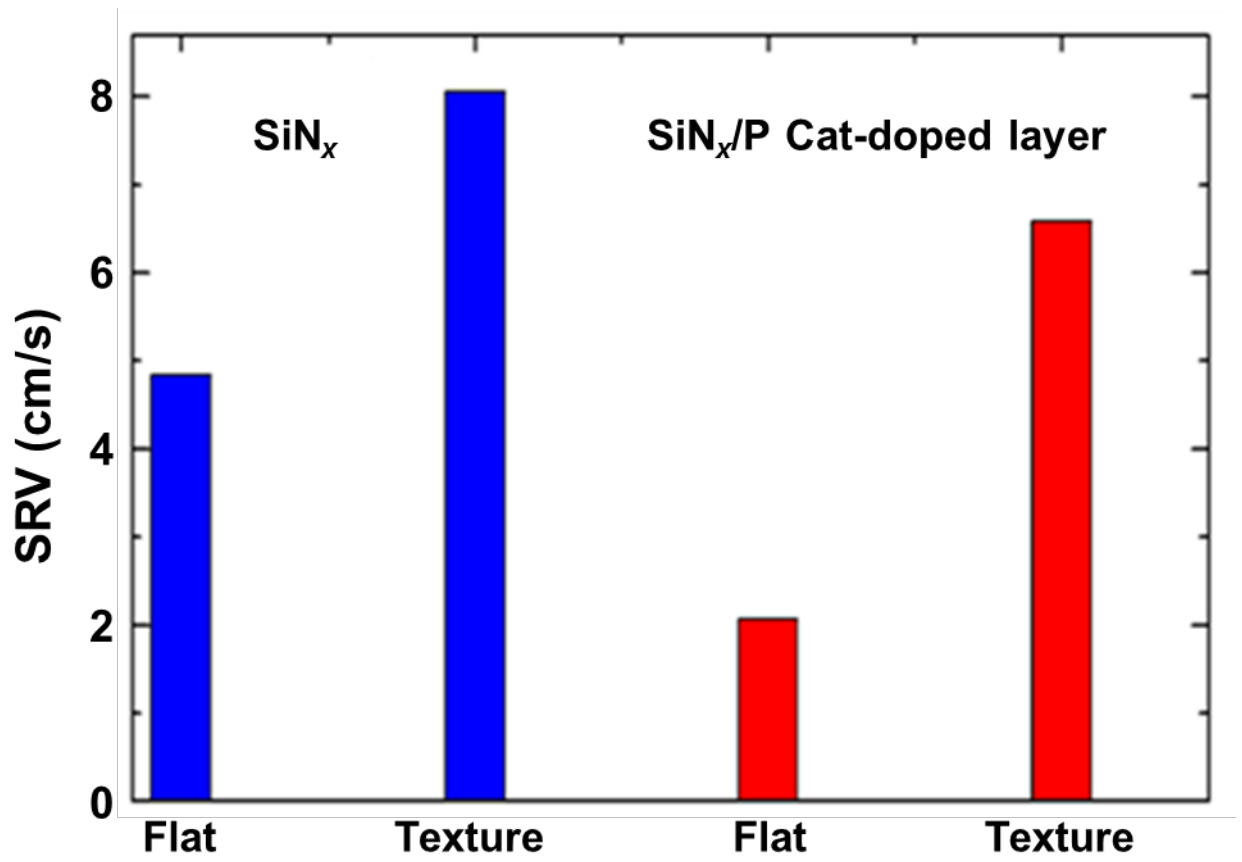


Fig. 6. (Color online)